Progress In Electromagnetics Research M, Vol. 99, 23–34, 2021

Analysis of Correlation between ROTI and S_4 Using GAGAN Data

Neelakantham Alivelu Manga[1, *], Kuruva Lakshmanna[1], Achanta D. Sarma[1], and Tarun K. Pant[2]

Abstract—As ionosphere is one of the most prominent sources of error, ionospheric TEC and scintillation studies are necessary for improving the performance of a navigation system. In this paper, the behavior of the correlation coefficient (ρ) between Rate of TEC Index (ROTI) and amplitude scintillation index (S_4) over low latitude station Hyderabad (Latitude: 17.44° (deg.) N, Longitude: 78.74° (deg.) E) for different seasons is analyzed. Also, the analysis is extended for nearly same longitude stations like Trivandrum, Bangalore, Bhopal, Delhi, and Shimla for the higher values of total $\mathbf{K_p}$ index for 60 days (most disturbed 5 days per month). For Trivandrum (lowest latitude station), it is observed that both S_4 and ROTI are high as compared to Bangalore, Bhopal, Delhi, and Shimla. It is found that there is a good correlation between the temporal variations of ROTI with S_4 after post sunset hours. The confidence intervals for computed correlation coefficients at 95% confidence level are also given.

1. INTRODUCTION

The performance of GPS is degraded by several errors including ionospheric scintillations. The stand-alone GPS is not suitable for certain critical navigation applications, such as aircraft landing. In order to meet the Required Navigation Performance (RNP) parameters: integrity, continuity, accuracy, and availability, Airport Authority of India (AAI) and Indian Space Research Organization (ISRO) developed regional Satellite Based Augmentation System (SBAS), called GPS Aided Geo Augmented Navigation (GAGAN) [1]. Ionospheric modelling is necessary for successful implementation of GAGAN system over Indian region. Total Electron Content (TEC) measurements have been used to study variability of the ionosphere during both geomagnetically quiet and disturbed conditions. A number of academic institutions and R & D organizations are involved in the process of understanding the structure and formation of ionospheric irregularities in the context of GAGAN based aviation applications. As the behaviour of the ionospheric irregularities is random in nature, statistical parameters are necessary to describe the randomness [2]. In this regard, Pi et al. [3] proposed an index called Rate of Total electron content Index (ROTI). TEC data from GAGAN network facilitate to characterize the ionospheric irregularities over Indian region.

As both large scale and small scale irregularities co-exist in equatorial irregularity structures, Basu et al. [4] reported that ROTI measurement can be used to predict the presence of scintillations causing those irregularities. Several other investigators also worked on this aspect [5–7]. They all inferred that large and small scale irregularities at scale size of a few kilometers and several hundred meters can be investigated simultaneously using ROTI and scintillation indices. Previous studies showed that there was certain correlation between ROTI and scintillation indices. Xiong et al. [8] estimated the correlation coefficient between ROTI and S_4 for different seasons and showed that there was a good correlation. In a recent research, correlation coefficient between ROTI and ionospheric scintillations (S_4

Received 14 October 2020, Accepted 12 November 2020, Scheduled 25 November 2020

* Corresponding author: Neelakantham Alivelu Manga (namanga04@gmail.com).

[1] Department of ECE, Chaitanya Bharathi Institute of Technology (CBIT), Gandipet, Hyderabad, Telangana State-500075, India.

[2] Space Physics Laboratory, VSSC, Thiruvananthapuram, Kerala, India.

and σ_ϕ) for geomagnetically disturbed and quiet days is analyzed for all visible satellites and individual satellites once a day [9]. The ionospheric scintillations and TEC vary with changes in season, geographic area, solar activity period, and time of the day. Hence, it is necessary to understand the correlation between ionospheric scintillations and TEC from time to time. In addition, the study of dynamics of ionospheric irregularities is important for analysing the space weather effects on GNSS.

In this paper, the correlation coefficient between ROTI and S_4 is estimated every 10 minutes interval after post sunset hours and analysed. Initially, the periods during which severe scintillations are identified, and for those periods the correlation coefficient between ROTI and S_4 is estimated and that too for individual satellites only. The present results correspond to a particular set of stations whose longitudes are nearly equal. So these results are unique to study the latitudinal behavior.

2. THEORETICAL BACKGROUND

The effects of ionospheric scintillations on the performance of GNSS receiver range from degradation of positioning accuracy to complete loss of signal lock. Therefore, identification of adverse ionospheric scintillation affects propagation paths, and their avoidance is helpful in maintaining uninterrupted positioning services [10].

2.1. Amplitude Scintillations

A radio wave traversing through ionospheric irregularities consisting of unstable plasma waves or small-scale electron density gradients will experience phase and amplitude fluctuations known as phase scintillations (σ_ϕ) and amplitude scintillations (S_4), respectively. In the case of phase scintillations, a sudden change in the phase may produce cycle slips and sometimes challenge a receiver's ability to hold lock on a signal. On the other hand, in the case of amplitude scintillations, degradation of the signal strength or even a loss-of-lock may occur requiring the receiver to attempt reacquisition of the satellite signal [11]. Scintillation effects are more severe during solar maximum years and in periods of heavy geomagnetic storms, mainly in equatorial and auroral regions. In mid-latitude regions, the occurrence of ionospheric scintillation is extremely rare. It happens only once or twice during the 11-year solar cycle [12, 13]. In equatorial regions, scintillations can be very strong and frequent, usually just after local sunset. S_4 and σ_ϕ indices are two parameters typically used to determine the level of scintillation activity.

Amplitude scintillation index (S_4) is defined as the standard deviation of signal intensity (SI) to the average signal intensity ($\langle \mathrm{SI} \rangle$). S_4 is a dimensionless number with a theoretical upper limit of 1.0, commonly estimated over an interval of 60 seconds. The total S_{4T}, including the effect of ambient noise, is given as [14, 15].

$$S_{4T} = \left(\frac{\langle \mathrm{SI}^2 \rangle - \langle \mathrm{SI} \rangle^2}{\langle \mathrm{SI} \rangle^2} \right)^{\frac{1}{2}} \tag{1}$$

In Equation (1), the received signal intensity SI is defined as the difference between the signal's Narrow-Band Power (NBP) and Wide-Band Power (WBP), measured over an interval of 20 ms as follows (Van Dierendonck et al., 1993 [16]):

$$\mathrm{WBP} = \sum_{i=1}^{20} \left(I_i^2 + Q_i^2 \right) \tag{2}$$

$$\mathrm{NBP} = \left(\sum_{i=1}^{20} I_i \right)^2 + \left(\sum_{i=1}^{20} Q_i \right)^2 \tag{3}$$

$$\mathrm{SI} = \mathrm{NBP} - \mathrm{WBP} \tag{4}$$

where I_i and Q_i samples represent 'in-phase' and 'quadra phase' of the accumulated samples.

To obtain the actual S_4 value, the effect of ambient noise and low frequency trend of SI must be removed [15]. After low pass filtering the signal intensity, the detrended normalized signal intensity

(SI_{det}) is calculated from

$$SI_{det}=\frac{SI}{(SI)_{LPF}}=\frac{NBP-WBP}{(NBP-WBP)_{LPF}} \tag{5}$$

For a given carrier-to-noise ratio (C/N_0) in dB-Hz, the signal to noise ratio (S/N_0) is related to C/N_0 as [16]

$$\frac{S}{N_0}=10^{\frac{C}{10N_0}} \tag{6}$$

The ambient noise in S_{4T} can be calculated as [15]

$$S_{4N_0}=\sqrt{\frac{100}{\frac{S}{N_0}}\left[1+\frac{500}{19\frac{S}{N_0}}\right]} \tag{7}$$

The effect of ambient noise on S_{4T} index is removed. The ambient noise free S_4 index can be expressed as,

$$S_4=\sqrt{\frac{\langle SI_{det}^2\rangle-\langle SI_{det}\rangle^2}{\langle SI_{det}\rangle^2}-\frac{100}{\frac{S}{N_0}}\left[1+\frac{500}{19\frac{S}{N_0}}\right]} \tag{8}$$

2.2. Rate of TEC Index (ROTI) and Its Relation with S_4

Ionosphere consists of electrons and electrically charged atoms around the earth from a height of 50 to more than 1000 km. It is ionized by solar and cosmic radiations during the day and night, respectively. TEC is the total number of electrons in a vertical column with a cross sectional area of 1 m^2 (one square meter). The Rate of TEC (ROT) is defined as [3]:

$$ROT(i) = STEC(i) - STEC(i-1) \tag{9}$$

where STEC (i) and STEC ($i-1$) are Slant Total Electron Content (STEC) at present instant 'i' and previous instant '$i-1$', respectively.

Rate of TEC Index (ROTI) is the standard deviation of ROT, is used to measure the ionospheric irregularity levels, and is expressed as [3, 9]

$$ROTI = \sqrt{\frac{1}{n}\sum_{i=1}^{n}\left(ROT\,(i)-\overline{ROT}\right)^2} \tag{10}$$

where n is the number of epochs or samples.

$\overline{ROT}$ is the mean of ROT.

Scale irregularities play an important role in describing the ionospheric behaviour. These scale irregularities are different for ROTI index and S_4 index. The scale length of ROTI represents large-scale ionospheric irregularities, while the scale-length of S_4 index represents the small-scale ionospheric irregularities [8].

The two parameters (ROTI and S_4) are indirectly related through Differential Rate of Total Electron Content Index (DROTI), by the following equation [17, 18].

$$S_4 = DROTI \cdot \frac{\lambda^2 r_e s}{2\pi v^2} \tag{11}$$

where $r_e = 2.8 \times 10^{-15}$ m is the radius of the electron, λ the wavelength of propagating signal, v a comprehensive velocity, and s the slant distance between the GNSS receiver and phase screen ionosphere pierce point,

$$DROTI = \sqrt{\frac{1}{n}\sum_{i=1}^{n}\left(DROT\,(i)-\overline{DROT}\right)^2} \tag{12}$$

and DROT (Differential Rate of TEC) is defined by

$$DROT = \frac{d}{dt}(ROT) \tag{13}$$

2.3. Estimation of Correlation Coefficient

The correlation between ROTI and S_4 can be quantified using the correlation coefficient ($\rho_{\mathrm{ROTI\,S_4}}$) and is defined as [19]

$$\rho_{\mathrm{ROTI\,S_4}} = \frac{\mathrm{C_{ROTI\,S_4}}}{\sigma_{\mathrm{ROTI}}\,\sigma_{\mathrm{S_4}}} \tag{14}$$

where $\mathrm{C_{ROTIS_4}}$ is the covariance, and σ_{ROTI} and $\sigma_{\mathrm{S_4}}$ are standard deviation of ROTI and S_4.

3. RESULTS AND DISCUSSIONS

Indian Regional Navigation Satellite System (IRNSS) is an autonomous satellite based navigation system designed, developed, and controlled by ISRO. IRNSS provides Position, Velocity, and Time (PVT) information over Indian region. It is designed to measure ionospheric delay precisely for every second. Novatel dual frequency GPS receivers (GSV4004B) are high data rate systems (≥ 50 Hz) and can record both TEC and ionospheric scintillations data (S_4 and σ_ϕ). On the other hand, IRNSS receiver is not capable of providing scintillations data. For ionospheric TEC measurements, under GAGAN program, Novatel Dual Frequency GPS receivers are placed all over India in 26 different locations for continuous data acquisition. For the present work, the data are provided by Space Application Centre (SAC), ISRO, and Ahmedabad. Based on Solar season's classification, the acquired data are segregated into 4 seasons namely vernal equinox (February, March, and April), summer solstice (May, June and July), autumn equinox (August, September, and October), and winter solstice (November, December, and January). The GAGAN TEC receiver data consist of 23 parameters, and out of these parameters only 7 parameters such as TOWC (sec), PRN, elevation angle (deg.), azimuth angle (deg.), $\mathrm{C/N_0}$ (dB-Hz), STEC (TECU), and total S_4 are used in the analysis. S_4 and STEC data with a sampling rate of 1 minute are considered. Initially, ROT is estimated, by subtracting the past sample from the present STEC sample (Equation (9)). The ROTI is calculated for 5 minutes data, and for the same period S_4 is averaged. Two such consecutive sets of values (ROTI and average of S_4) are used for computing correlation coefficient (ρ). For this, an optimum sample size of 10 observations is selected as it results in better resolution than with a sample size of 20 observations.

The confidence intervals of correlation coefficients for all the considered stations for a given confidence level are estimated. In the process, to have a meaningful observation, a threshold of 0.5 is considered, and all the correlation coefficients above this threshold are taken into consideration for the estimation of confidence intervals.

Not all the receivers are equipped with a provision to directly measure scintillations. Even if they are, they are very costly. Therefore, our present studies go a long way in analysing the behaviour of scintillations using TEC values obtained from a relatively economical receiver. Previously, these studies are not carried out simultaneously in multiple directions from a fixed station. This will help in studying the spatial variations at the same time. It is expected that these observations can be used to investigate the ionospheric scintillations over Indian region using an IRNSS receiver. The data of Hyderabad TEC receiver (Latitude: 17.44° N, Longitude: 78.74° E) during the period of 1 January to 30 November 2016 are considered. Correlation coefficient is estimated every 10 minutes interval of time after post sun hours (18 : 30 to 22 : 00 IST hrs.) for quiet and disturbed days. In order to avoid multipath effect, higher elevation angles ($> 30°$) are considered [9].

3.1. Analysis of Correlation Coefficient on Disturbed Days for Various Seasons

While correlation between S_4 index and ROTI is analyzed, it is important to note that this correlation is relevant to a particular Ionospheric Pierce Point (IPP) in the space [20, 21]. IPP is the intersection point of line of sight from satellite to receiver at an altitude of 350 km above the surface of the Earth. Even though the receiver stations are static, the Medium Earth Orbit (MEO) GPS satellites rotate around the earth with a speed of 3.9 km/s due to which the IPPs keep changing with respect to time.

For the analysis, five (05) most disturbed days per month, i.e., 60 days per year which have higher values of the total K_p index are considered for Hyderabad station ((https://www.gfz-potsdam.de/en/ kpindex/; http://wdc.kugi.kyoto-u.ac.jp/kp /index.html). The

planetary 3-hour-range index K_p is the mean standardized K-index from 13 geomagnetic observatories between 44 degrees and 60 degrees northern or southern geomagnetic latitude. It is derived from the maximum fluctuations of horizontal components observed on a magnetometer during a three-hour interval. For each disturbed day, correlation coefficient is analyzed during the period of 18:30 to 22:00 IST hrs, and results are shown in Table 1. From the table, it is observed that seasonally S_4 has good correlation with ROTI in Vernal equinox, Autumnal equinox, and Winter solstice as compared to Summer solstice. Also, it is observed that the correlation coefficient is strong ($\rho = 0.95$) in March (Vernal equinox) and weak (ρ =0.24) in August (autumn equinox). For a disturbed day (7 March 2016) ($3 \leq K_p \leq 5$), after post sunset hours (18:30 to 22:00 IST hrs), the results of ROTI, S_4 index, and correlation coefficient along with IPP location are presented in Figure 1. Correlation coefficient is weak at low elevation angles and strong at higher elevation angles. The maximum correlation coefficient is observed between 21:00 and 21:10 IST hrs. Also, the corresponding computed confidence intervals are given in Table 3.

Table 1. Analysis of correlation coefficient between ROTI and S_4 for disturbed days.

S. No.	Season	Month	Date	K_p index	PRN	Max of ρ
1	Vernal Equinox	February	18	$4 \leq K_p \leq 5$	07	0.82
2		March	07	$3 \leq K_p \leq 5$	28	0.95
3		April	13	$3 \leq K_p \leq 5$	06	0.70
4	Summer Solstice	May	08	$3 \leq K_p \leq 6$	02	0.45
5		June	05	$2 \leq K_p \leq 5$	05	0.42
6		July	07	$3 \leq K_p \leq 5$	29	0.80
7	Autumn Equinox	August	04	$2 \leq K_p \leq 4$	18	0.24
8		September	03	$4 \leq K_p \leq 6$	10	0.75
9		October	25	$3 \leq K_p \leq 6$	31	0.88
10	Winter Solstice	November	25	$2 \leq K_p \leq 5$	03	0.70
11		January	21	$3 \leq K_p \leq 6$	09	0.74

Table 2. Analysis of correlation coefficient between ROTI and S_4 for quiet days.

S. No.	Season	Month	Date	K_p index	PRN	Max of ρ
1	Vernal Equinox	February	22	$0 \leq K_p \leq 1$	07	0.22
2		March	13	$0 \leq K_p \leq 2$	28	0.29
3		April	19	$0 \leq K_p \leq 1$	06	0.44
4	Summer Solstice	May	25	$0 \leq K_p \leq 1$	02	0.24
5		June	03	$0 \leq K_p \leq 1$	05	0.10
6		July	27	$0 \leq K_p \leq 2$	29	0.52
7	Autumn Equinox	August	28	$0 \leq K_p \leq 1$	18	0
8		September	16	$0 \leq K_p \leq 2$	10	0.55
9		October	11	$0 \leq K_p \leq 1$	31	0.28
10	Winter Solstice	November	19	$0 \leq K_p \leq 1$	19	0.62
11		January	25	$0 \leq K_p \leq 1$	09	0.49

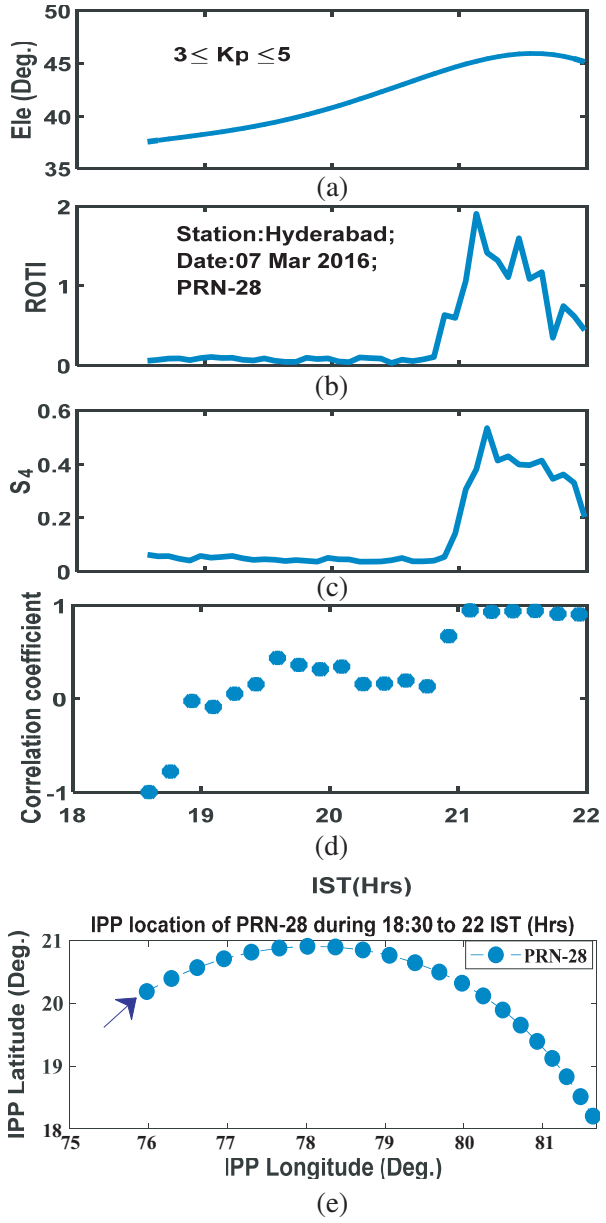

Figure 1. Variations of various parameters with respect to time for the date on 07 March 2016 (disturbed day) at Hyderabad GAGAN receiver station; (a) Elevation angle (deg.), (b) ROTI, (c) S_4, (d) correlation coefficient between ROTI and S_4 and (e) IPP location.

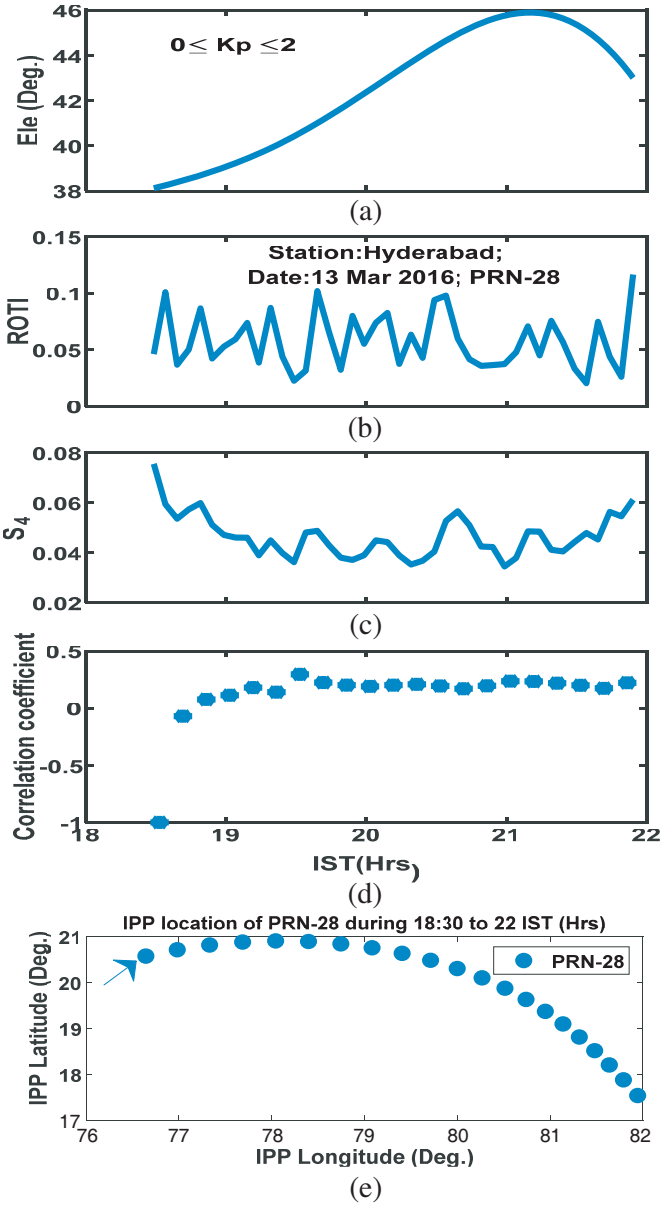

Figure 2. Variations of various parameters with respect to time for the date on 13 March 2016 (quiet day) at Hyderabad GAGAN receiver station; (a) Elevation angle (deg.), (b) ROTI, (c) S_4, (d) correlation coefficient between ROTI and S_4 and (e) IPP location.

3.2. Analysis of Correlation Coefficient on Quiet Days for Various Seasons

Correlation analysis of quiet day ($0 \leq K_p \leq 2$) (13 March 2016) data is done for a period of 18:30 to 22:00 IST hrs, and the results are shown in Figure 2. It is found that the maximum correlation coefficient (0.29) occurred between 19:30 to 19:40 IST hrs. Similarly, the correlation coefficient analysis is done for 50 quiet days of the remaining 10 months. However, only 10 days results of maximum correlation coefficient are presented in Table 2. It is observed that S_4 has weak correlation with ROTI

Table 3. Confidence intervals of correlation coefficient at a confidence level of 95% for various stations during post sunset hours for selected disturbed days.

Sl. No.	GAGAN Receiver Station	Date	PRN of Satellite Vehicle	Confidence Intervals
1	Hyderabad	07 March 2016	28	0.88–0.90
2	Trivandrum	20 January 2016	03	0.42–0.83
3	Bangalore	02 November 2016	26	0.87–0.92
4	Bhopal	09 December 2016	16	0.34–0.47
5	Delhi	23 December 2016	23	0.46–0.66
6	Shimla	28 September 2016	14	0.65–0.75

for quiet days in all seasons.

From these results, it is concluded that correlation coefficient is high for earth geomagnetic disturbed days ($3 \leq K_p \leq 6$) as compared to quiet days ($0 \leq K_p \leq 2$).

3.3. Analysis of Correlation Coefficient for Nearly Same Longitude Stations ($\sim 77^0 \pm 0.7^0$)

In the present analysis, five approximately same longitude TEC receiver stations namely Trivandrum (8.49° N, 76.90° E), Bangalore (12.95° N, 77.68° E), Bhopal (23.28° N, 77.34° E), Delhi (28.56° N, 77.22° E), and Shimla (31.08° N, 77.06° E) are considered as shown in Figure 3. Out of the available one-year data and based on K_p index, the most disturbed days of 60, 55, 12, 10, and 60 are identified for Trivandrum, Bangalore, Bhopal, Delhi, and Shimla stations, respectively.

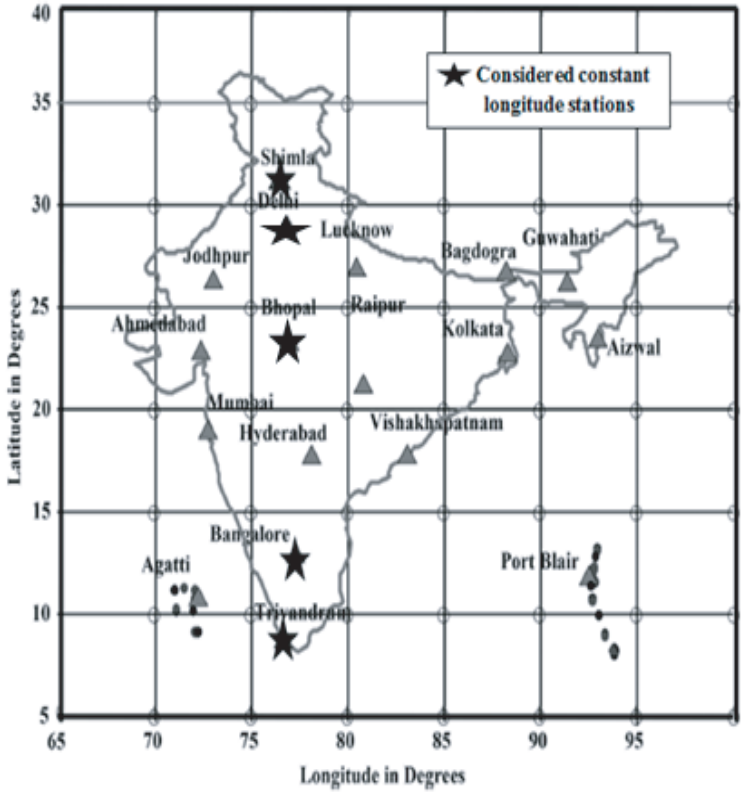

Figure 3. Location of GAGAN TEC receivers over Indian region.

For the identified data, correlation coefficient is analysed after post sunset hours during the period of 18:00 to 20:00 IST hrs. As both S_4 and STEC are a function of earth geomagnetic disturbance index (K_p) values, from the analysis, it is observed that S_4 has good correlation with ROTI for higher values of S_4 and weak correlation for low values of S_4.

3.3.1. Trivandrum (8.49° N, 76.90° E)

Correlation coefficient between ROTI and S_4 is analysed for Trivandrum which is the lowest latitude station among the considered stations. It is observed that the correlation coefficient is good for the data corresponding to the period of higher values of S_4 and ROTI and is low for lower values of S_4 and ROTI. Out of the most disturbed 60 days, the maximum value of ROTI and S_4 is observed on 20th January 2016 (total $K_p = 28$) for PRN 3.

For this day, C/N_0, ROTI, S_4, correlation coefficient, and IPP location are plotted in Figure 4. The maximum correlation coefficient occurs (0.70) during the period of 19:90 to 20:00 IST hrs. It

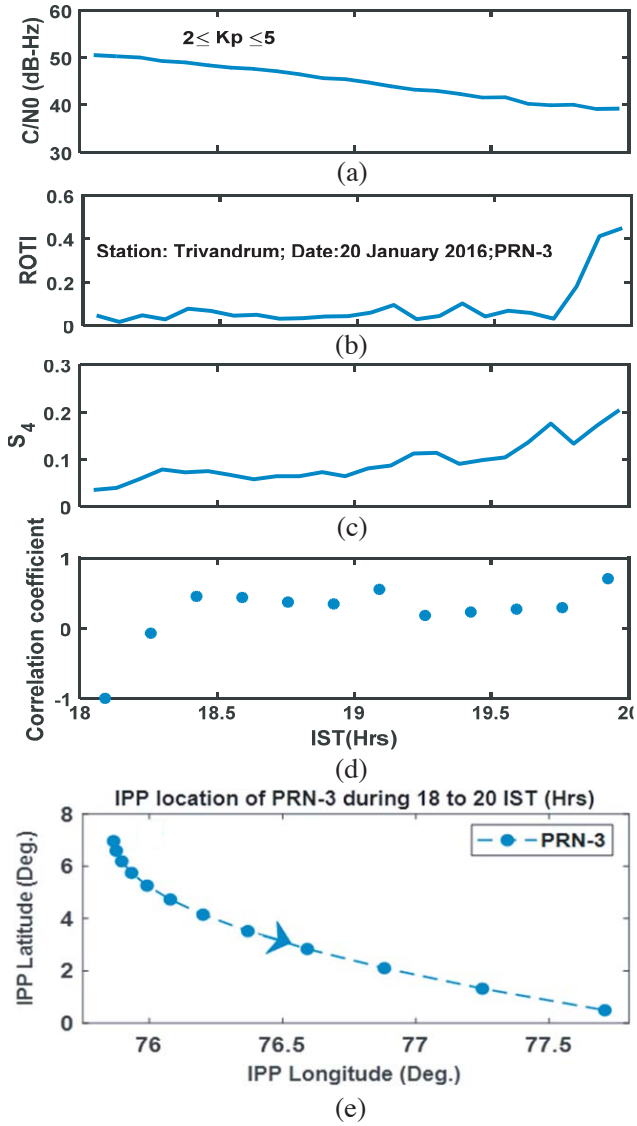

Figure 4. Variations of various parameters with respect to time for the date on 20 January 2016 at Trivandrum GAGAN receiver station; (a) C/N_0, (b) ROTI, (c) S_4, (d) correlation between ROTI and S_4 and (e) IPP Location.

is interesting to note that S_4 is inversely proportional to C/N_0, and good temporal consistency of correlation coefficient exists during 18:40 to 19:50 IST hrs.

3.3.2. Bangalore (12.95° N, 77.68° E)

For Bangalore station, it is found that the maximum values of S_4 and ROTI occurred on 02 November 2016 (total K_p = 21+) for PRN-26. The correlation coefficient is maximum (ρ = 0.92) during the period 19:40 to 19:50 IST hrs as shown in Figure 5.

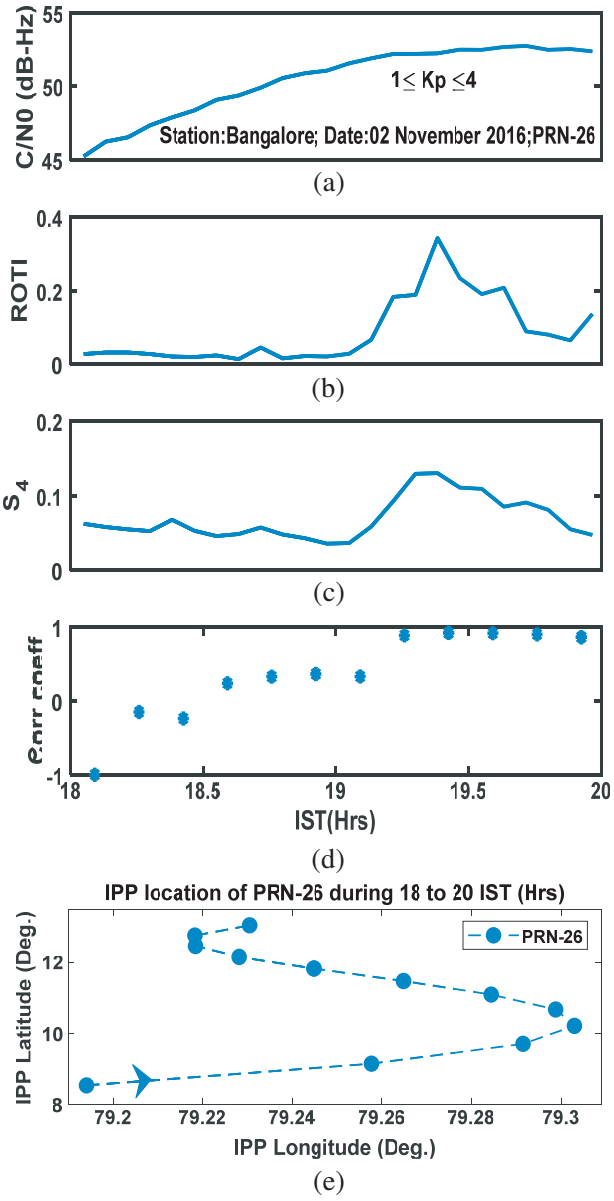

Figure 5. Variations of various parameters with respect to time for the date on 2 November 2016 at Bangalore GAGAN receiver station; (a) C/N_0, (b) ROTI, (c) S_4, (d) correlation between ROTI and S_4 and (e) IPP Location.

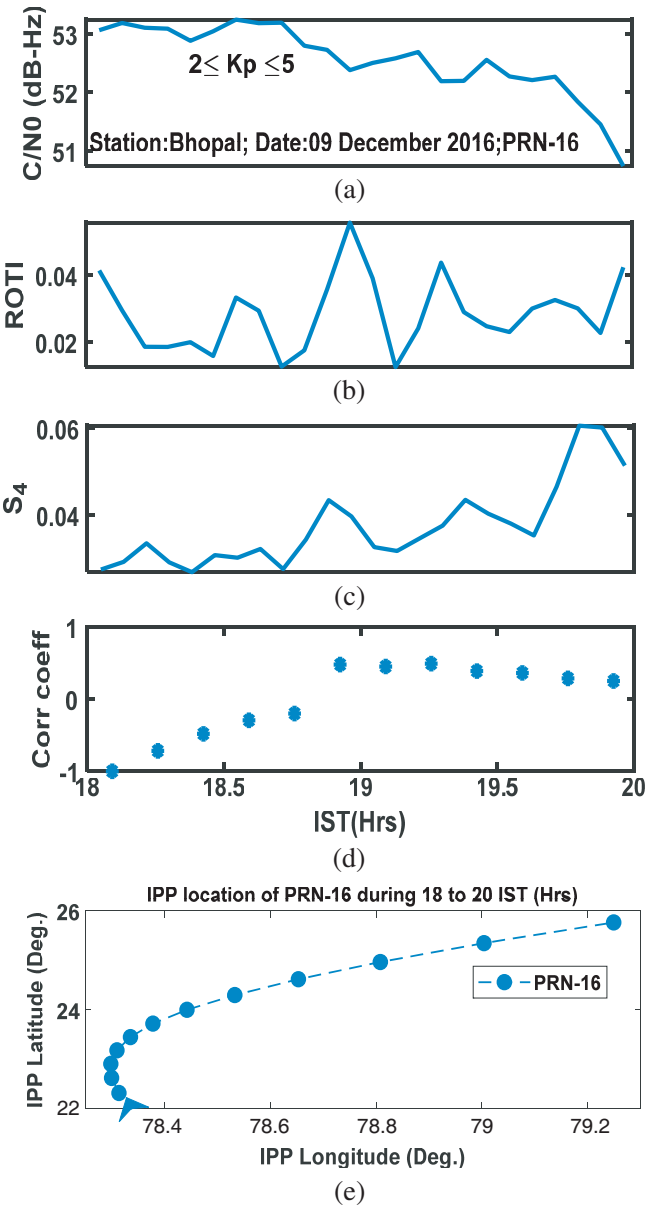

Figure 6. Variations of various parameters with respect to time for the date on 09 December 2016 at Bhopal GAGAN receiver station; (a) C/N_0, (b) ROTI, (c) S_4, (d) correlation between ROTI and S_4 and (e) IPP Location.

3.3.3. Bhopal (23.28° N, 77.34° E)

For Bhopal station, it is found that the maximum values of S_4 and ROTI occurred on 09 December 2016 (total $K_p = 29$) for PRN-16. The correlation coefficient is maximum ($\rho = 0.4887$) during the period 18:80 to 18:90 IST hrs as shown in Figure 6.

3.3.4. Delhi (28.56° N, 77.22° E)

For Delhi station, it is found that the maximum values of S_4 and ROTI occurred on 23 December 2016 (total $K_p = 27$) for PRN-23. The correlation coefficient is maximum ($\rho = 0.633$) during the period 18:30 to 19:40 IST hrs as shown in Figure 7.

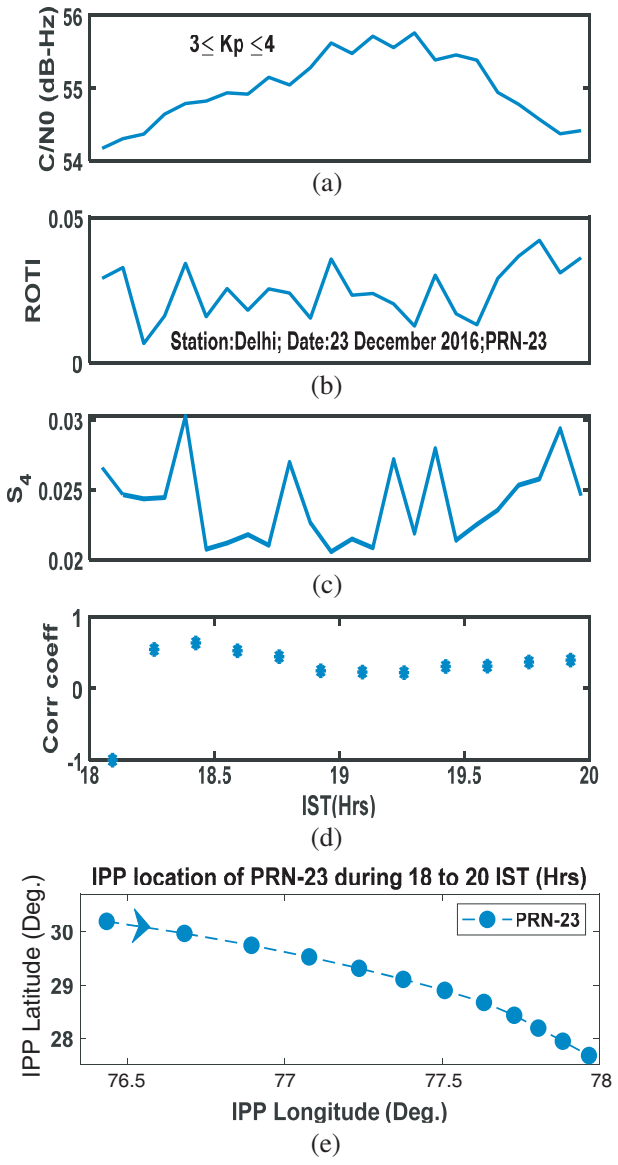

Figure 7. Variations of various parameters with respect to time for the date on 23 December 2016 at Delhi GAGAN receiver station; (a) C/N_0, (b) ROTI, (c) S_4, (d) correlation between ROTI and S_4 and (e) IPP location.

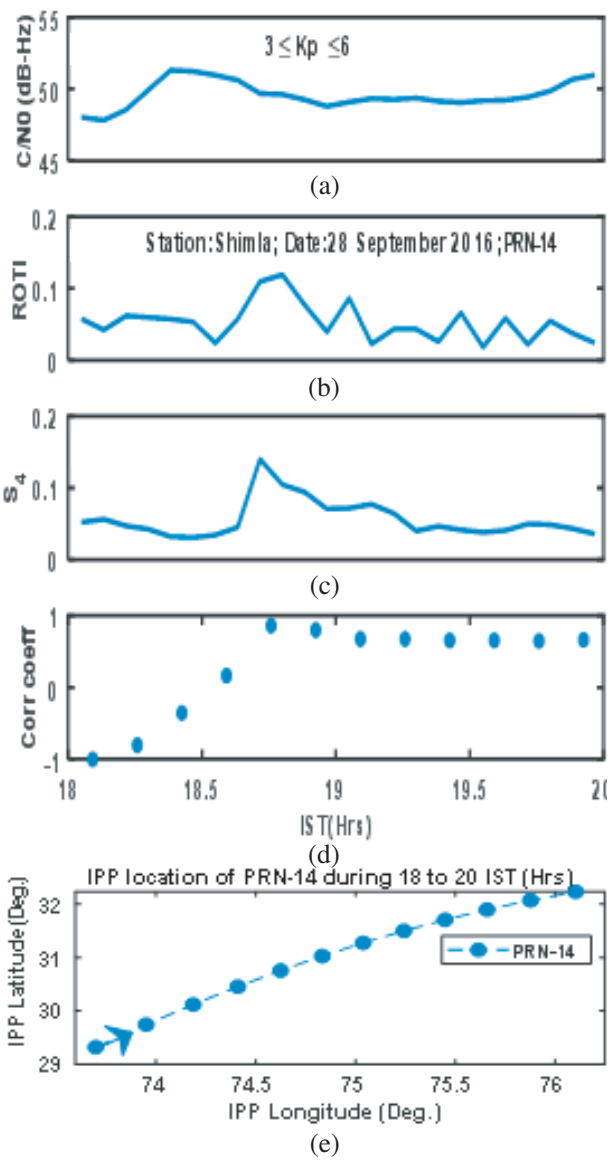

Figure 8. Variations of various parameters with respect to time for the date on 28 September 2016 at Shimla GAGAN receiver station; (a) C/N_0, (b) ROTI, (c) S_4, (d) correlation between ROTI and S_4 and (e) IPP location.

3.3.5. Shimla (31.08° N, 77.06° E)

For Shimla station, the maximum values of S_4 and ROTI occurred on 28 September 2016 (total $K_p = 35+$). The correlation coefficient is maximum ($\rho = 0.86$) during 18:70 to 18:80 IST hrsas shown in Figure 8. Temporal consistency between ROTI and S_4 during the period of 19:20 to 20:00 IST hrs is also observed.

From the analysis it is found that whenever S_4 value is high, higher correlation between S_4 and ROTI is observed at low IPP latitudes. However, for Bhopal, as the scintillation value is not high, the correlation values are not significant even for the low IPP latitudes.

4. CONCLUSION

A comprehensive analysis of correlation coefficient between ROTI and S_4 is carried out in this paper. Correlation coefficient between ROTI and S_4 is estimated for quiet and disturbed days of 4 seasons over Hyderabad station. It is found that the correlation coefficient is high during disturbed days as compared to quiet days for all seasons. A maximum correlation coefficient of 0.95 is observed on 07 March 2016 (Vernal equinox) which is positive. Positive value of correlation coefficient implies that the variations of S_4 follow that of ROTI w.r.t. time, and it shows the strength of a relationship between the two values. This is helpful in estimating the ionospheric scintillations. On the other hand, negative value implies an inverse correlation between them. This is an indication that the two variables move in the opposite directions. The confidence interval estimated for this is in the range of 0.88 to 0.90 for a confidence level of 95%. The minimum correlation coefficient of 0.24 is observed on 04 August 2016 (autumn equinox). Further, it is noticed that a weak correlation is at lower elevation angles and strong at high elevation angles. On the other hand, it is observed that there is no significant correlation on quiet days. The correlation coefficient for approximately same longitude stations (Trivandrum, Bangalore, Bhopal, Delhi, and Shimla) is also estimated. It is found that the correlation coefficient is good during the period of higher values of ROTI and S_4 and vice versa. A good temporal consistency of correlation coefficient for Trivandrum station as compared to Bangalore, Bhopal, Delhi, and Shimla stations is also found. Further, it is noticed that the intensity of scintillations and ROTI is less with increasing latitudes except for Shimla station due to the high values of $K_p\,(3 \leq K_p \leq 6)$ index. The intensity of scintillations is more for Trivandrum station, as it is closer to geomagnetic equator which further confirms earlier reported findings [22, 23].

ACKNOWLEDGMENT

The work presented in this paper has been carried out under the project entitled "A Local Short Model for Forecasting Ionospheric Scintillations for GNSS Applications over Indian Region" sponsored by RESPOND, ISRO Bangalore, vide sanction letter no:ISRO/RES/2/399/15-16, dated: 13 July 2015.

REFERENCES

1. Kumar, A., A. D. Sarma, A. K. Mondal, and K. Yedukondalu, "A wide band antenna for multi-constellation GNSS and augmentation systems," *Progress In Electomgnetics Research M*, Vol. 11, 65-77, 2010.
2. Srinivas, S., A. D. Sarma, and H. K. Achanta, "Modeling of ionospheric time delay using anisotropic IDW with jackknife technique," *IEEE Transactions on Geoscience and Remote Sensing*, Vol. 54, No. 1, 513–519, Jan. 2016.
3. Pi, X., A. Mannucci, U. Lindqwister, and C. Ho, 1997, "Monitoring of global ionospheric irregularities using the worldwide GPS network," *Geophysical Research Letters*, Vol. 24, No. 18, 2283–2286, 1997.
4. Basu, S., K. Groves, J. Quinn, and P. Doherty, 1999, "A comparison of TEC fluctuations and scintillations at Ascension Island," *J. Atmos. Solar Terr. Phys.*, Vol. 61, No. 16, 1219–1226, 1999.

5. Wang, J. and Y. (Jade) Morton, "Spaced multi-GNSS receiver array as ionosphere radar for irregularity drift velocity estimation during high latitude ionospheric scintillation," *30th International Technical Meeting of the Satellite Division of the Institute of Navigation (ION GNSS+2017)*, 3389–3401, Portland, Oregon, September 25–29, 2017.
6. Alfonsi, L., L. Spogli, J. Tong, G. De Franceschi, V. Romano, A. Bourdillon, M. Le Huy, C. N. Mitchell, "GPS scintillation and TEC gradients at equatorial latitudes in April 2006," *Adv. Space Res.*, Vol. 47, No. 10, 1750–1757, 2011.
7. Seif, A., M. Abdullah, A. Marie Hasbi, and Y. Zou, "Investigation of ionospheric scintillation at UKM station, Malaysia during low solar activity," *Acta Astronaut.*, Vol. 81, No. 1, 92–101, 2012.
8. Xiong, B., W.-X. Wan, B.-Q. Ning, H. Yuan, and G.-Z. Li, "A comparison and analysis of the S_4 index, C/N and Roti over Sanya," *Chinese J. Geophys.*, Vol. 50, No. 6, 1414–1424, 2007.
9. Zhe, Y. and Z. Liu, "Correlation between ROTI and Ionospheric Scintillation Indices using Hong Kong low latitude GPS dara," *GPS Solutions*, 2015.
10. Yedukondalu, K., A. D. Sarma, and V. Satya Srinivas, "Estimation and mitigation of GPS multipath interference using adaptive filtering," *Progress In Electromagnetics Research M*, Vol. 21, 133–148, 2011.
11. Conker, R. S., M. B. El Arini, C. J. Hegarty, and T. Hsiao, "Modeling the effects of ionospheric scintillation on GPS/SBAS availability," *Radio Sci.*, Vol. 38, No. 1, 2003.
12. Klobuchar, J. A. 1991, "Iospheric effects on GPS," GPS world.
13. Klobuchar, J. A. and P. H. Doherty Klobuchar, 2000, "A look ahead: Expected ionospheric effects on GPS," *GPS Solutions*, Vol. 2, No. 1, 42–48, 2000.
14. Sunda, S., S. Yadav, R. Sridharan, M. S. Bagiya, P. V. Khekale, P. Singh, and S. V. Satish, "SBAS-derived TEC maps: A new tool to forecast the spatial maps of maximum probable scintillation index over India," *GPS Solutions*, Vol. 21, 1469–1478, 2017.
15. Van Dierendonck, A. J., Q. Hua, P. Fenton, and J. Klobuchar, "Commercial ionospheric scintillation monitoring receiver development and test results," *Proc. of the ION 52nd Annual Meeting*, 1996.
16. Van Dierendonck, A. J., J. Klobuchar, and Q. Hua, "Ionospheric scintillation monitoring using commercial single frequency C/A code receivers," *Proceedings of ION GPS-93*, Salt Lake City, UT, 1993.
17. Rino, C. L., "A power law phase screen model for ionospheric scintillation: 1. Weak scatter," *Radio Science*, Vol. 14, No. 6, 1135–1145, 1979.
18. Liu, Y. and S. Radicella, "On the correlation between ROTI and S_4," *Annales Geophysicae Discussions*, 2019, https://doi.org/10.5194/angeo-2019-147.
19. Bendat, J. S. and A. G. Piersol, "Random data analysis and measurement procedures," A Wiley-Interscience, 1986.
20. Ravichandra, K., V. Satya Srinivas, and A. D. Sarma, "Investigation of ionospheric gradients for GAGAN applications," *Earth Planets Space Journal*, Vol. 61, 633–635, 2009, ISSN: 1880-5981.
21. Klobuchar, J. A., "Ionospheric time-delay algorithm for single-frequency GPS users," *IEEE Transactions on Aerospace and Electronics Systems*, Vol. 23, 325–331, 1987.
22. Aarons, J., "Global morphology of ionospheric scintillation," *Proc. of the IEEE*, Vol. 70, 360–378, 1982.
23. Venkateswarlu, G. and A. D. Sarma, "A new technique based on grey model for forecasting of ionospheric GPS signal delay using GAGAN data," *Progress In Electromagnetics Research M*, Vol. 59, 33–43, 2017.